Transition from modulated to exploding dissipative solitons: Hysteresis, dynamics, and analytic aspects

Orazio Descalzi[1,2,*] and Helmut R. Brand[2]

[1]*Complex Systems Group, Facultad de Ingeniería y Ciencias Aplicadas, Universidad de los Andes, Av. San Carlos de Apoquindo 2200, Santiago, Chile*

[2]*Department of Physics, University of Bayreuth, 95440 Bayreuth, Germany*

(Received 26 March 2010; published 9 August 2010)

We investigate the properties of and the transition to exploding dissipative solitons as they have been found by Akhmediev's group for the cubic-quintic complex Ginzburg-Landau equation. Keeping all parameters fixed except for the distance from linear onset, μ, we covered a large range of values of μ from very negative values to $\mu=0$, where the zero solution loses its linear stability. We find, with increasing values of μ, stationary pulses, pulses with rapid oscillations, and pulses modulated with an additional small frequency. The transition to exploding solitons arises via a hysteretic transition involving symmetric and asymmetric pulses with two frequencies. As μ is increased in the regime of exploding solitons, the fraction of symmetric exploding solitons is increasing. At the transition from asymmetric two frequency pulses to exploding solitons, only asymmetric exploding solitons are found. We completed our analysis with an analytic study of the collapse time for the exploding solitons and found good agreement with our numerical results.

DOI: 10.1103/PhysRevE.82.026203 PACS number(s): 82.40.Bj, 05.70.Ln, 42.65.Sf, 47.20.Ky

I. INTRODUCTION AND MOTIVATION

To model stable localized solutions (particle- or holelike) in macroscopic pattern-forming dissipative systems different avenues of approach have been used. One is the direct numerical solution of the underlying macroscopic basic equations, such as, for example, in the case of the localized states for the convection in binary fluid mixtures the hydrodynamic equations [1], or for surface reactions the associated reaction-diffusion equations [2]. The other main approach is to apply prototype equations such as envelope equations [3,4] (frequently applicable near the onset of an instability [5–7]) or order parameter equations [8–11], which take into account the symmetries of the system to be described [7,12]. In both cases the idea is to have an approach that is useful, at least qualitatively, for more than one specific system. From an experimental point of view stable pulses and/or stable holes have been observed for systems as diverse as binary fluid convection [13–15], slot convection [16–19], the Faraday instability in various complex fluids [20], in chemical reactions [21,22], in particular on surfaces [21] as well as for various optical systems [23].

Envelope equations are derived systematically near the onset of an instability via a reduced perturbation expansion in the distance from instability onset as a small parameter [5–7]. They are obtained from the underlying macroscopic basic equations, such as hydrodynamic equations, for example, for simple fluids, binary fluid mixtures or nematic liquid crystals, as well as reaction-diffusion equations used to describe chemical reactions in spatially extended systems. The cubic-quintic complex Ginzburg-Landau (CGL) equation studied in the following is a prototype equation applicable near the weakly hysteretic onset of an oscillatory instability to traveling or standing waves [24]. Sometimes, as for example for convection in binary fluid mixtures, envelope equations can only be used for qualitative comparisons, since boundary layers arise [15].

For the cubic-quintic CGL equation, as a prototype envelope equation, many different types of stable pulse- [3,4,25–47] and holelike [42–45,48,49] solutions have been found and analyzed. These various types of localized solutions have been called dissipative solitons [25] in order to emphasize that they arise for strongly driven and damped dissipative systems in contrast to classical solitons for which driving and damping is typically taken into account only perturbatively [6].

One has also investigated the influence of different boundary conditions on many types of pulses and hole solutions. In addition to the numerically most frequently implemented periodic boundary conditions the physically important Neumann and Dirichlet boundary conditions have been examined [48,50–52].

One type of dissipative solitons with outstanding properties that set it apart from other dissipative solitons are explosive dissipative solitons (called originally eruptive solitons) [26,53–56]. They are found in the regime of anomalous dispersion. Among the features that have been well characterized is the stable existence of symmetric and asymmetric explosive solitons over a wide range of two parameters (the real part of the cubic nonlinearity and the imaginary part of the quintic nonlinearity) in the cubic-quintic CGL equation [26,53,56], their experimental observation in nonlinear optics [54] and a number of features, which are similar to dynamical systems [55,56].

In the present study we keep all parameters fixed except for the bifurcation parameter (the distance from linear onset). Here we study the transitions involving explosive solitons and other stable solutions (pulsating dissipative solitons with two vastly different frequencies and space-filling homogeneous solutions) and the associated hysteresis effects. In addition, we present an analytic estimate of the collapse time

*odescalzi@miuandes.cl

and we point out many differences in behavior when compared to simple dynamical systems with a small number of degrees of freedom.

Thus explosive dissipative solitons are a rather complex spatiotemporal object. As a function of time they undergo several changes: they start with an unstable pulse shedding radiation or "phonons" [26,53], then in one of the wings of the unstable pulse perturbations grow to generate another pulselike object, these two pulses—both unstable—interact and form a rather broad, high and highly unstable pulse. In a last step the latter collapses [26,53] to form the unstable pulse reminiscent in shape of the stable fixed shaped pulse found first by Thual and Fauve [3]. The overall behavior is characterized by a cycle time that fluctuates around an average and by high frequency oscillations leading to radiation over most of the average cycle time of an explosive dissipative soliton.

The paper is organized as follows. In the next section we describe the model and the numerical technique used. In Sec. III we describe our numerical and analytic results followed in Sec. IV by a comparison with previous results on explosive dissipative solitons and in Sec. V by discussion and conclusions.

II. MODEL

We investigate the complex subcritical cubic-quintic Ginzburg-Landau equation in one spatial dimension,

$$\partial_t A = \mu A + (\beta_r + i\beta_i)|A|^2 A + (\gamma_r + i\gamma_i)|A|^4 A + (D_r + iD_i)\partial_{xx} A, \tag{1}$$

where $A(x,t)$ is a complex field. In writing down this equation we have already transformed into the moving frame. To guarantee saturation to quintic order, γ_r is taken to be negative, while $\beta_r > 0$ to have a weakly inverted bifurcation. The diffusion coefficient, D_r is assumed to be positive. In the spirit of an envelope equation, the fast spatial and temporal variations have already been split off when writing down the envelope equation. To compare with measurable quantities such as, for example, temperature variations in fluid dynamics, these rapid variations must be taken into account [5,7,24].

TABLE I. Conversion of the coefficients of the two versions of the cubic-quintic Ginzburg-Landau equation used here versus the one used in nonlinear optics

Present notation	Nonlinear optics
μ	δ
β_r	ε
β_i	1
γ_r	μ
γ_i	ν
D_r	β
D_i	$D/2$

To facilitate the comparison with the notation used in the field of nonlinear optics, we write down the cubic-quintic complex Ginzburg-Landau equation in the notation frequently used in optics [25,26]

$$i\psi_z + \frac{D}{2}\psi_{tt} + |\psi|^2\psi + \nu|\psi|^4\psi = i\delta\psi + i\varepsilon|\psi|^2\psi + i\beta\psi_{tt} + i\mu|\psi|^4\psi. \tag{2}$$

Comparing Eqs. (1) and (2) we can make the identifications listed in Table I.

In the following we use periodic boundary conditions for A. Recent studies of the influence of Neumann [51] and Dirichlet [52] boundary conditions have shown that these do no affect qualitatively nonmoving pulses, regardless whether these are breathing or not, provided the box size is large enough compared to the pulse width at its maximum extent. We expect the same to hold for exploding solitons.

Most of our numerical and analytic studies were carried out for the same parameter values as in the plots of the pioneering papers of Akhmediev's group on exploding solitons [26,53], which read in the present notation $\beta_r=1$, $\gamma_r=-0.1$,

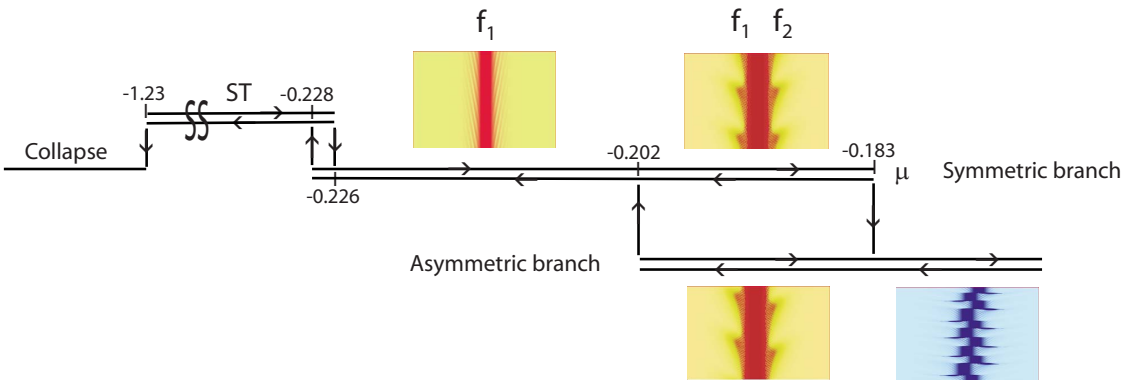

FIG. 1. (Color online) Phase diagram: the various types of localized states are shown as a function of the bifurcation parameter, μ. The other parameters investigated are: $\beta_r=1$, $\beta_i=0.8$, $\gamma_r=-0.1$, $\gamma_i=-0.6$, $D_r=0.125$, $D_i=0.5$, $dx=0.08$, and $dt=0.005$. As μ is increased one obtains first stationary pulses (ST), followed by oscillating pulses with one frequency (f_1) and by a hysteretic transition to pulses with two frequencies (f_1, f_2), which can be either symmetric or asymmetric. As μ is increased beyond $\mu=-0.183$ exploding solitons arise stably until the linear threshold $\mu \equiv 0$ is reached.

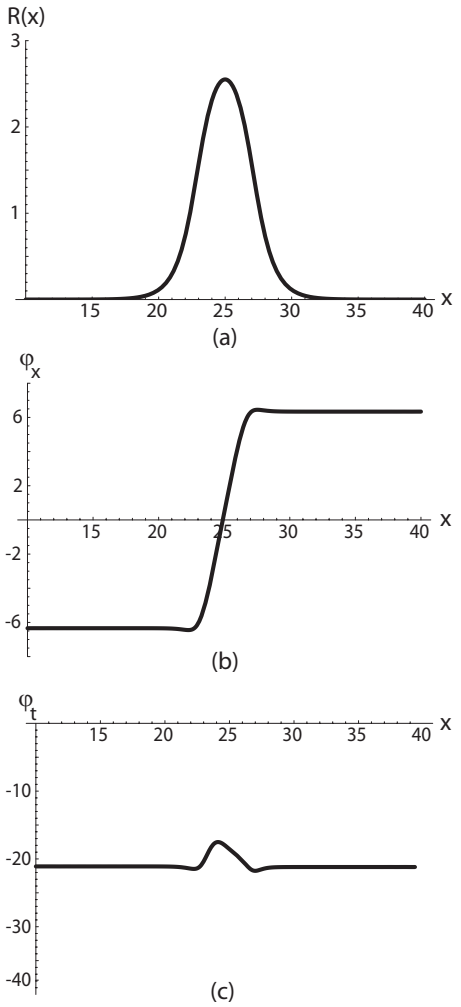

FIG. 2. The figures show a stationary stable pulse for $\mu=-0.25$, $\beta_i=1.0$, $dx=0.2$ and $dt=0.01$: (a) snapshot of the modulus $R(x)\equiv|A(x)|$ and (b) snapshot of the local wave vector φ_x as a function of space, and (c) the local frequency φ_t as a function of space. The qualitative behavior of the local wave vector and of the local frequency as functions of space will be used below in an analytic calculation to estimate the collapse time of exploding solitons. The other parameter values are as for Fig. 1.

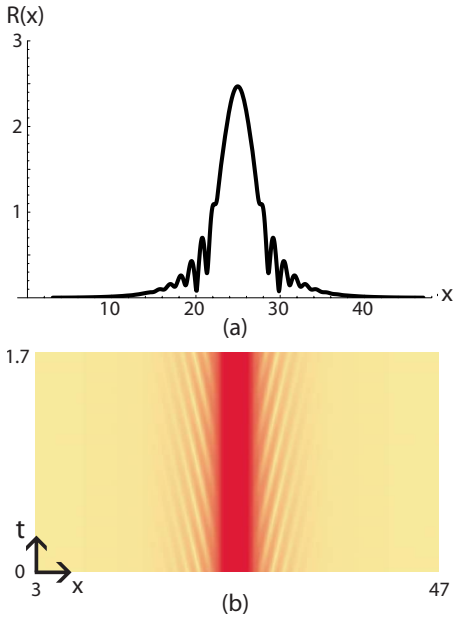

FIG. 3. (Color online) The figures show a stable pulse oscillating with one frequency (denoted by regime f_1 in Fig. 1) for $\mu=-0.21$ and $\beta_i=0.8$ (a) snapshot of the modulus $R(x)$ and (b) $x-t$ plot for a total time of $T=1.7$ (340 iterations) in the limit of long times showing rapid oscillations when compared to the much slower modulations discussed below. One clearly sees the radiation or "phonons" coming off the wings in the $x-t$ plot. The other parameter values are as for Fig. 1.

$\gamma_i=-0.6$, $D_r=0.125$, and $D_i=0.5$. For β_i we use in the figures shown $\beta_i=0.8$ (for Figs. 1 and 3) and $\beta_i=1$ (for all other figures). Thus the only parameter value varied in the present study is μ, the distance from linear onset. We varied μ from $\mu=-1.5$ (a value below the range, where localized structures are stable solutions of the cubic-quintic CGL equation) to $\mu=0$, the value where $A=0$ loses linear stability. In this sense the avenue of our approach is different from previous work on exploding solitons, where μ was typically held fixed. Instead two other parameters β_r and γ_i were varied revealing a rather large range for the stable existence of exploding solitons for variations in these two parameters [26,53].

Explicit fourth order Runge-Kutta finite differencing was used as numerical method. We used a constant box size $L=Ndx=50$ and varied the grid spacing dx as well as the time step dt. The number N was adjusted to achieve a constant box size L. To validate our numerical method, the grid spacing dx was varied between $dx=0.2$ and $dx=0.04$ and the time step dt between $dt=0.01$ and 0.002. We thus varied both, the grid spacing dx and the time step dt, by a factor of 5 to verify that all results presented in the following were not sensitive to this discretization. For periodic boundary conditions we have $A(0)=A(L)$.

We would also like to stress that increasing the accuracy the 'phase diagram' is slightly shifted in the $\mu-\beta_i$ plane, but that the observed sequence ST—$f_1-(f_1-f_2)$—explosions is robust.

III. RESULTS

A. Numerical results

To analyze the transitions shown by exploding solitons we investigated all localized patterns as a function of the bifurcation parameter, μ. As discussed in the last section, all other parameter values in the cubic quintic complex Ginzburg-Landau equation have been kept at a fixed value. For sufficiently negative values of μ only the solution $R(x)\equiv|A(x)|=0$ is stable. This situation prevails below the saddle node.

As μ is increased above $\mu\sim-1.23$ stable localized pulses of the type described first by Thual and Fauve [3] arise and dominate until $\mu\sim-0.227$ (compare Fig. 1). In Fig. 2 we have plotted the modulus $R(x)$ (a) and the local wave vector $\varphi(x)$ (b), which is static, as a function of x. In addition, we have plotted in (c), φ_t, the time derivative of the phase, which is constant everywhere except inside the core of the pulse. In the analytic analysis given below, the constant part

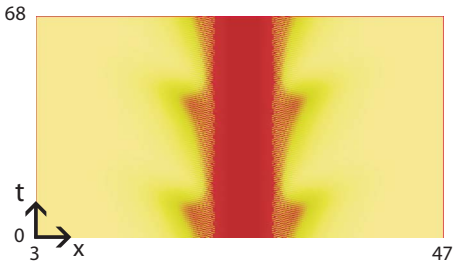

FIG. 4. (Color online) The figure shows the $x-t$ plot of a stable pulse oscillating symmetrically with two frequencies (denoted by regime f_1-f_2 symmetric branch in Fig. 1) for $\mu=-0.19$, $\beta_i=1.0$, $dx=0.2$, and $dt=0.01$ in the asymptotic time regime. The total time shown is $T=68$ (corresponding to 6800 iterations) clearly revealing the much slower time scale of the modulations. The other parameter values are as for Fig. 1.

of φ_t will be denoted as Ω. The qualitative features of these three plots will be used in the next subsection on analytic results to derive an estimate for the collapse time observed for exploding solitons.

As μ is increased, one finds for the window between $\mu \sim -0.227$ and $\mu \sim -0.202$ oscillating dissipative solitons characterized by one rather large and fixed frequency. These oscillations are accompanied by radiation or "phonons" coming off the wings of the oscillating dissipative soliton. This phenomenon can be seen very clearly in the $x-t$ plot shown in Fig. 3 for $\mu=-0.21$. We note that the time scale on this $x-t$ plot is about two orders of magnitude smaller than on the other $x-t$ plots shown below to bring out clearly the details of the rapid oscillations. To prepare our snapshots and $x-t$ plots for all time-dependent states we waited for a sufficiently long time until no further qualitative changes in the dissipative solitons were detectable. We will call in the following this behavior the "asymptotic time regime." The transition from the stationary pulse to the oscillating pulse with one frequency shows a hysteresis of size $\Delta\mu \approx 0.002$ around $\mu=-0.227$, which is comparable to the step size with which we have varied the bifurcation parameter μ.

As the value of μ is increased, slow temporal modulations arise giving rise to a state characterized by two frequencies, which are vastly different (by about two orders of magnitude). As revealed by the $x-t$ plot shown in Fig. 4, the slow

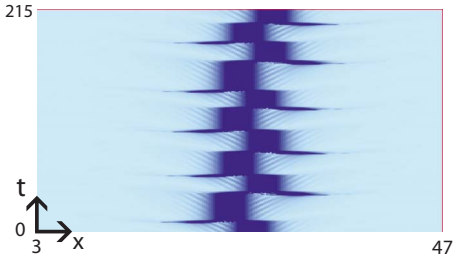

FIG. 5. (Color online) The figure shows the $x-t$ plot of an asymmetric exploding pulse for $\mu=-0.17$, $\beta_i=1.0$, $dx=0.2$, and $dt=0.01$ in the asymptotic time regime. The total time shown is $T=215$ (corresponding to 21 500 iterations) clearly revealing the alternating nature of the explosions. The other parameter values are as for Fig. 1.

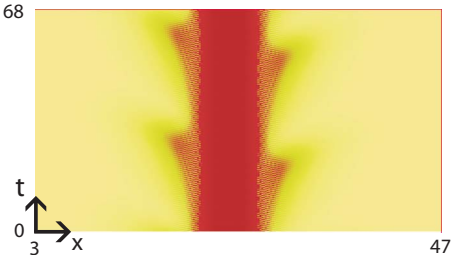

FIG. 6. (Color online) The figure shows the $x-t$ plot of a stable pulse oscillating asymmetrically with two frequencies (denoted by regime f_1-f_2 asymmetric branch in Fig. 1) for $\mu=-0.19$, $\beta_i=1.0$, $dx=0.2$, and $dt=0.01$ in the asymptotic time regime. The total time shown is $T=68$ (corresponding to 6800 iterations) again clearly revealing the much slower time scale of the modulations—similar to Fig. 4. The other parameter values are as for Fig. 1.

modulations occur symmetrically in space—the regime denoted as f_1-f_2 symmetric branch in Fig. 1. We note that there is no hysteresis for the transition from the oscillating pulse with one frequency (f_1) to the oscillating pulse with two frequencies (f_1-f_2).

When μ is increased above $\mu \sim -0.183$ a qualitative change arises and the regime of exploding solitons is reached (Fig. 5). In the asymptotic time regime we find close to, but above $\mu \sim -0.183$ exclusively asymmetric exploding solitons. We would like to stress that there is no net motion of the location of the exploding solitons in the long time limit. The apparent slow motion of this location to the right in Fig. 5 is due to the rather short time interval shown in the $x-t$ plot. Before we turn to a thorough discussion of the detailed spatiotemporal behavior of exploding solitons and of symmetric exploding solitons, we finish the overview of the types of behavior occurring in the "phase diagram" shown in Fig. 1. When reducing the value of μ from above $\mu \sim -0.183$ to values below $\mu \sim -0.183$, the asymmetric exploding solitons make a transition to a state, which is also asymmetric and characterized by two frequencies. This behavior is brought out clearly in the $x-t$ plot shown in Fig. 6 and is

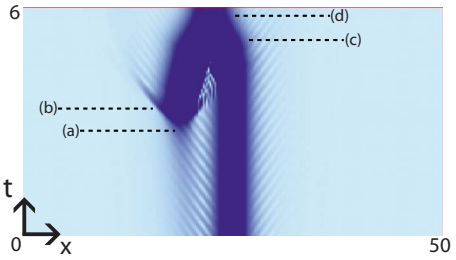

FIG. 7. (Color online) The figure shows the blow-up of the $x-t$ plot of an asymmetric exploding pulse for $\mu=-0.17$, $\beta_i=1.0$, $dx=0.2$, and $dt=0.01$ already shown in Fig. 5 for one asymmetric explosion. Here the total time shown is $T=6$ (corresponding to 600 iterations). The labels (a), (b), (c), and (d) denote four characteristic instants in time for the evolution of an asymmetric exploding soliton: (a): start of the peak growing in the wing of the main peak, (b): maximum of the width of the side peak and start of the interaction with the main peak, (c): maximum width of the single peak after the interaction just before the beginning of the collapse, (d): asymptotic shape of the peak before the beginning of the next growth cycle.

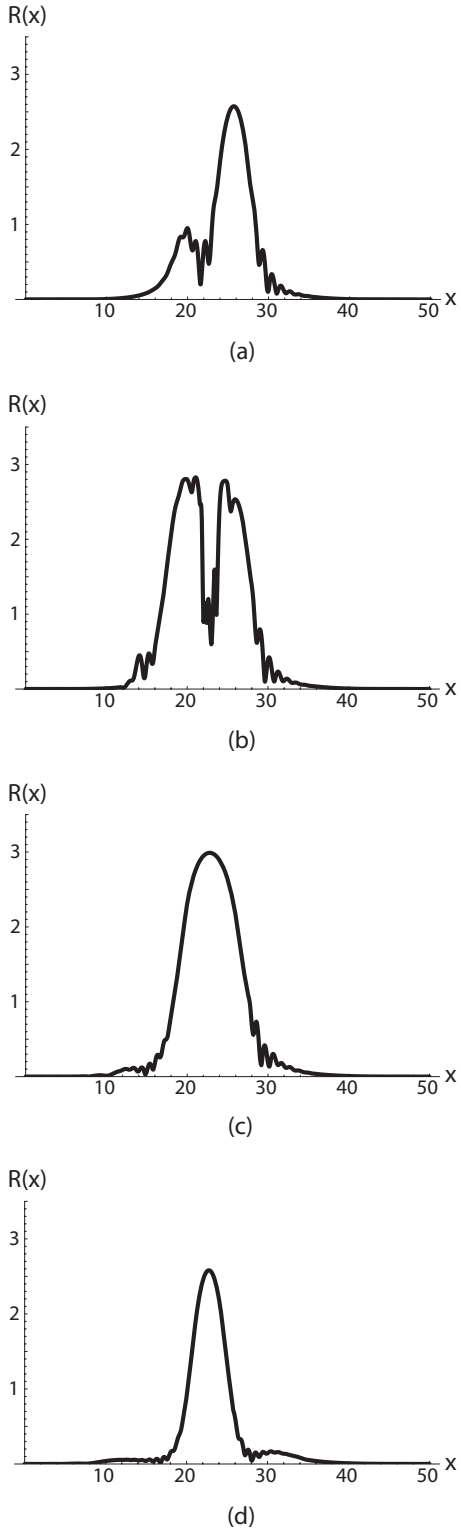

FIG. 8. Four snapshots during one life cycle of an asymmetric exploding soliton for $\mu=-0.17$, $\beta_i=1.0$, $dx=0.2$, and $dt=0.01$. The location in time of the four snapshots shown has already been denoted by (a), (b), (c), and (d) in Fig. 7.

denoted as the asymmetric f_1-f_2 branch in Fig. 1.

Reducing μ on the asymmetric f_1-f_2 branch leads at $\mu \sim -0.202$ to a transition back to the state characterized by one rapid frequency only. Thus we have hysteretic behavior between asymmetric and symmetric behavior for the f_1-f_2 branches in the regime $\sim -0.202 < \mu < \sim -0.183$.

To characterize asymmetric solitons in some detail we have plotted in Fig. 7 part of one life cycle of an asymmetric exploding dissipative soliton and in Fig. 8 four snapshots taken at characteristic instances in time during one life cycle. Notice that as shown in Fig. 5 the cycle time of one explosion ("life cycle") varies randomly around a value close to 21.5. For an exploding soliton one has not only radiation or 'phonons' as in the case of the oscillating dissipative solitons shown in Figs. 3, 4, and 6. In addition, one has a perturbation growing in the wings of the original dissipative soliton above a certain threshold size [location (a) in the $x-t$ plot in Figs. 7 and 8(a)]. This side peak grows in magnitude and interacts with the previous main peak and reaches a maximum width of the compound object. This instant in time is denoted as (b) in Fig. 7 and shown as a snapshot in Fig. 8(b). As a consequence of the interaction one peak with a fixed maximum width results [shown as location (c) in Fig. 7 and as a snapshot in Fig. 8(c)], which in turn collapses rather rapidly to a state similar, but shifted in space compared to the original starting peak. Since this starting peak as well as the final peak in one life cycle are also both unstable, the same cycle starts again, which leads to a fairly well defined repeat time, which we have called the life cycle. It turns out that the collapse time between the two states indicated in Figs. 7(c) and 7(d) and shown as plots in Figs. 8(c) and 8(d) can be calculated quite accurately by approximate analytic techniques as we will demonstrate in the next subsection. We would like to emphasize that the rather rapid spatial variations of the modulus in Figs. 3 and 8 are not due to the spatial grid spacing used, but are rather due to the nature of the exploding solitons. We have checked this carefully by varying the grid spacing for both figures by a factor of 5.

As the bifurcation parameter μ is increased, we find in the asymptotic time regime first only asymmetric exploding solitons over a substantial range in μ and then alternating periods of asymmetric exploding solitons and symmetric exploding solitons starting at a threshold value $\mu \sim -0.075$. As μ is increased further and as eventually the linear threshold $\mu=0$ is reached (compare the two snapshots shown in Fig. 9), the fraction of space-filling patterns in the whole box is increasing and leads to a filling-in in the long time limit and thus to a spatially homogeneous pattern at $\mu \equiv 0$.

In Fig. 10 we have quantified the total number of explosions for symmetric and asymmetric exploding dissipative solitons as a function of μ for a fixed time interval $T=600$ (60 000 iterations) in the asymptotic time regime. Two main features emerge: (a) the total number of explosions increases almost linearly as μ is increased toward zero; and (b) the number of symmetric explosions also increases approximately linearly as μ is increased above $\mu \sim -0.075$.

B. Analytic results

It is always interesting (and important) to see to what extent experimental and/or numerical results can be obtained by analytical calculations. Equation (1), which has been studied numerically above, can be written as

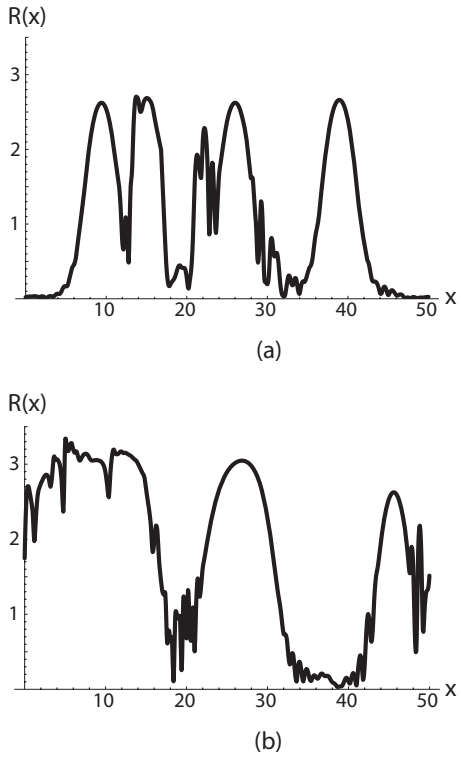

FIG. 9. Two snapshots of spatiotemporal structures for $\mu=0$, $\beta_i=1.0$, $dx=0.2$, and $dt=0.01$ that is as the linear threshold is approached. In this case the fraction of the box filled by spatiotemporal structures is very large even in a large box, eventually leading to a filling-in and thus to a spatially homogeneous state in the long time limit.

$$R_t = \mu R + \beta_r R^3 + \gamma_r R^5 + D_r(R_{xx} - R\varphi_x^2) - D_i(R\varphi_{xx} + 2R_x\varphi_x), \tag{3}$$

$$R\varphi_t = \beta_i R^3 + \gamma_i R^5 + D_r(R\varphi_{xx} + 2R_x\varphi_x) + D_i(R_{xx} - R\varphi_x^2), \tag{4}$$

by replacing the complex field $A(x,t)$ by its polar representation $A(x,t)=R(x,t)\exp\{i\varphi(x,t)\}$. In Sec. III it has been mentioned that from $\mu\sim-1.23$ until $\mu\sim-0.227$ we obtain stationary pulses whose modulus R and local wave vector φ_x are static. In addition, φ_t turns out to be also static and even constant everywhere except inside the core of the pulse. Thus, such stationary localized structures can be viewed approximately as rigid bodies rotating at fixed frequency Ω around the x axis. Figure 2 shows the modulus, local wave vector and frequency for a stationary pulse at $\mu=-0.25$. Then for the stationary pulse we can replace the phase $\varphi(x,t)$ by $\Omega t+\theta(x)$, where θ_x is the static local wave vector. After some algebra Eqs. (3) and (4), for this case, reduce to [57]

$$0 = \mu_+ R + \beta_+ R^3 + \gamma_+ R^5 + R_{xx} - R\theta_x^2, \tag{5}$$

$$\mu_- R = \beta_- R^3 + \gamma_- R^5 + R\theta_{xx} + 2R_x\theta_x, \tag{6}$$

where

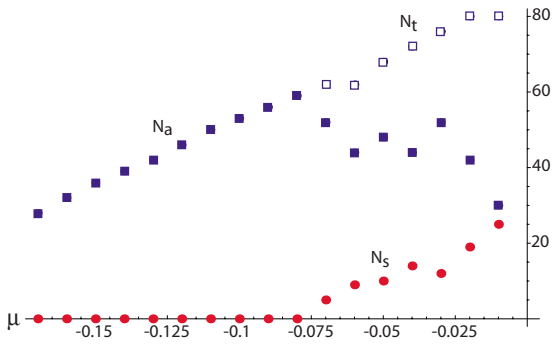

FIG. 10. (Color online) This plot shows the number of explosions of an exploding soliton for a fixed time interval in the asymptotic time limit as a function of the bifurcation parameter, μ. Here N_t (open squares) denotes the total number of explosions with $N_t=N_a+2N_s$ where N_a (solid squares) and N_s (solid circles) denote the number of asymmetric and symmetric explosions, respectively. Two main features emerge: (a) the total number of explosions is growing, as the linear threshold is approached, approximately linearly and (b) above a threshold value for μ symmetric explosions start and also increase in number roughly linearly for growing values of μ.

$$\mu_+ = \frac{D_r\mu - D_i\Omega}{|D|^2}; \quad \beta_+ = \frac{D_r\beta_r + D_i\beta_i}{|D|^2},$$

$$\gamma_+ = \frac{D_r\gamma_r + D_i\gamma_i}{|D|^2}; \quad \mu_- = \frac{D_i\mu + D_r\Omega}{|D|^2},$$

$$\beta_- = \frac{D_r\beta_i - D_i\beta_r}{|D|^2}; \quad \gamma_- = \frac{D_r\gamma_i - D_i\gamma_r}{|D|^2},$$

and $|D|^2=D_r^2+D_i^2$.

In spite of the nonlinearities involved in Eqs. (5) and (6) we can calculate the frequency Ω by noticing that the local wave vector θ_x is constant ($\theta_x=+p$ for $R_x<0$ and $\theta_x=-p$ for $R_x>0$) outside the core of the pulse [see Fig. 2(b)], in particular for $R\ll 1$. Thus Eqs. (5) and (6) become linearized,

$$0 = \mu_+ R + R_{xx} - Rp^2, \tag{7}$$

$$\mu_- R = -2pR_x\,\mathrm{sgn}(R_x), \tag{8}$$

The above equations imply the following relation to be satisfied:

$$0 = \mu_+ - p^2 + \frac{\mu_-^2}{4p^2}. \tag{9}$$

Solving this equation for Ω we obtain finally,

$$\Omega = -\frac{1}{D_r^2}[D_i(\mu D_r - 2p^2|D|^2) + 2p|D|^2\sqrt{-\mu D_r + p^2|D|^2}]. \tag{10}$$

Evaluating this expression for $\mu=-0.25$, $\beta_r=1$, $\beta_i=1$, $\gamma_r=-0.1$, $\gamma_i=-0.6$, $D_r=0.125$, $D_i=0.5$, and $p=6.34$ [value obtained directly from Fig. 2(b)] we get $\Omega=-21.06$. From Fig. 2(c) we see that this analytical result is in very good agree-

ment with the numerical calculation, which gives −21.10.

To estimate the collapse time of an exploding dissipative pulse, that is, the time the pulse needs to pass from a maximum [see state (c) in Figs. 7 and 8] to a minimum width [see state (d) in Figs. 7 and 8], we study the relaxational dynamics in the wings of a stationary pulse. From Eqs. (3) and (4) the dynamics of a slightly perturbed modulus in the wings ($R \ll 1$) reduce to

$$R_t = \frac{|D|^2}{D_r}[(\mu_+ - p^2)R + R_{xx}]. \tag{11}$$

Notice that the above system can be derived from a Lyapounov potential (compare, for example, Ref. [58] for a review of the notion of nonequilibrium potential for systems far from equilibrium),

$$R_t = -\frac{\delta\Phi}{\delta R}, \tag{12}$$

where

$$\Phi = \int \left\{ \frac{|D|^2}{2D_r}[(p^2 - \mu_+)R^2 + R_x^2]dx \right\}. \tag{13}$$

From the above expressions clearly the fast dynamics is given by the $k=0$ perturbations so that the collapse time is given by

$$t_{collapse} \sim \frac{D_r}{|D|^2(p^2 - \mu_+)}. \tag{14}$$

Evaluating this expression for $\mu=-0.25$, and using the above indicated parameters $t_{collapse}$ results to be close to 0.7. From Fig. 7 we see that the collapse time for exploding dissipative solitons is ~0.68.

IV. COMPARISON WITH PREVIOUS RESULTS ON EXPLOSIVE SOLITONS

The pioneering work on exploding (first denoted as erupting) dissipative solitons by the group of Akhmediev [26,53] demonstrated the stable existence of symmetric exploding solitons as well as their occurrence over a rather large range of the parameters β_r and γ_i. As β_r is reduced, symmetric exploding solitons were found to either become periodic solutions or to collapse completely. As β_r was increased, symmetric exploding solitons were replaced by chaotic or stationary pulses. Shortly thereafter Cundiff and colleagues [54] provided experimental evidence for soliton explosions in a Ti:sapphire mode-locked laser in a study combined with a numerical investigation of a model closely related to the experiment.

Later on these studies were used as a starting point to investigate the bridge to dynamical systems [55,56], in particular to Shilnikov's theorem, incorporating a linear stability analysis. It was also pointed out that there is a number of differences to the case of exploding solitons because of the fact that the cubic quintic complex Ginzburg-Landau equation is a system with an infinite number of degrees of freedom and not a dynamical system with a small (three in Shilnikov's case) number of degrees of freedom. In addition, it was pointed out in Ref. [56] that stable strongly asymmetric soliton explosions can arise for a small region inside the parameter space where symmetric explosions occur.

The approach here has been quite complementary to the one used before. We kept all the parameters at the values used in Refs. [26,53] for preparing the $x-t$ plots, except for the distance from linear onset, μ, the bifurcation parameter in the context of the onset of instabilities, for example, in fluid systems and for chemical reactions. We covered all values of μ from the collapse of all pulse solutions at very negative values of μ (for which only $A=0$ is known to be a stable solution), all the way to $\mu=0$, where the zero solution loses its linear stability and where instead space-filling solutions with $|A|=$const. prevail. In between we find, with increasing values of μ, stationary pulses, pulses with one rapid frequency oscillation, and pulses modulated with an additional small frequency. When μ is varied the transition to exploding solitons arises via a hysteretic transition involving symmetric and asymmetric pulses with two frequencies. As μ is increased in the regime of exploding solitons, the fraction in time of symmetric exploding solitons is increasing above another threshold in the overall regime of stable exploding dissipative solitons. At the transition from the asymmetric two frequency pulses to exploding solitons, only asymmetric exploding solitons are found. We did not observe purely symmetric exploding solitons in the long time limit for the range of parameters studied here. We completed our analysis with an analytic study of the collapse time for the exploding solitons and found good agreement with the results of our numerical investigations.

V. DISCUSSION AND CONCLUSIONS

Here we have presented the results of our studies on the dynamics and transitions shown by exploding dissipative solitons. All investigations were performed changing only the bifurcation parameter measuring the distance from linear onset. Previously it had already been shown [26,53] that exploding dissipative solitons exist over a substantial range of values of the quintic refractive index and of the value of the cubic destabilizing coupling in the cubic-quintic complex Ginzburg-Landau equation. As major results the following features emerge. First of all we find that exploding dissipative solitons arise from modulated oscillatory dissipative solitons characterized by two frequencies via a hysteretic transition involving symmetrically as well as asymmetrically modulated dissipative solitons. The latter two in turn arise from an oscillatory branch showing rather fast oscillations. Within the stable regime of exploding solitons we find for increasing bifurcation parameter first exclusively asymmetric exploding solitons and only above a threshold value of the bifurcation parameter we find sequences of symmetric and asymmetric exploding dissipative solitons of various durations alternating as a function of time in the asymptotic time regime. A statistical analysis shows that both, the total number of soliton explosions as well as the number of symmetric soliton explosions, increases approximately linearly with the value of the bifurcation parameter as the latter is increased

toward linear onset. When linear onset is reached, the spatially homogeneous solution with a fixed modulus is obtained in the long time limit.

In addition, we have demonstrated that approximate analytic calculations give almost quantitative agreement with our numerical results for the collapse time associated with the time scale between the maximum and the minimum width of the pulse of the exploding dissipative solitons.

A detailed comparison with previous work on exploding solitons shows that our results are almost completely complementary, but coincide in the region of overlap. Naturally we do not expect the phenomenon of exploding dissipative solitons to be confined to the cubic-quintic complex Ginzburg-Landau equation, but to arise equally well for corresponding order parameter equations of Swift-Hohenberg type as well as for suitable reaction-diffusion equations. This expectation is, in particular, based on our previous work pointing out a number of similarities for different types of localized solutions of such prototype equations [8,11,59–62].

While our analysis has been performed for periodic boundary conditions, we expect it to be equally applicable for Dirichlet and Neumann boundary conditions, since previous work on these boundary conditions has indicated that stationary or breathing localized solutions can accommodate Dirichlet or Neumann boundary conditions essentially unchanged provided the box size is large compared to the maximum width reached for the localized, non-propagating solutions [51,52].

Clearly it is highly desirable to see experimental tests of the predictions presented here. Since one has already investigated exploding solitons in optics [54], it will be natural to check for the transitions and the dynamical properties studied here in optical systems. Possible additional experimental systems include autocatalytic chemical reactions and binary fluid convection.

ACKNOWLEDGMENTS

O.D. wishes to acknowledge the support of FAI (Universidad de los Andes, 2010). H.R.B. thanks the Deutsche Forschungsgemeinschaft for support of this work through the Forschergruppe FOR 608. “Nichtlineare Dynamik komplexer Kontinua.”

[1] W. Barten, M. Lücke, and M. Kamps, Phys. Rev. Lett. **66**, 2621 (1991).
[2] M. Bär, M. Eiswirth, H. H. Rotermund, and G. Ertl, Phys. Rev. Lett. **69**, 945 (1992).
[3] O. Thual and S. Fauve, J. Phys. (France) **49**, 1829 (1988).
[4] H. R. Brand and R. J. Deissler, Phys. Rev. Lett. **63**, 2801 (1989).
[5] A. C. Newell and J. A. Whitehead, J. Fluid Mech. **38**, 279 (1969).
[6] A. C. Newell, *Solitons in Mathematics and Physics* (Society for Industrial and Applied Mathematics, Philadelphia, 1985).
[7] M. C. Cross and P. C. Hohenberg, Rev. Mod. Phys. **65**, 851 (1993).
[8] H. Sakaguchi and H. R. Brand, Physica D **97**, 274 (1996).
[9] H. Sakaguchi and H. R. Brand, EPL **38**, 341 (1997).
[10] H. Sakaguchi and H. R. Brand, J. Phys. II **7**, 1325 (1997).
[11] H. Sakaguchi and H. R. Brand, Physica D **117**, 95 (1998).
[12] J. Swift and P. C. Hohenberg, Phys. Rev. A **15**, 319 (1977).
[13] P. Kolodner, Phys. Rev. A **44**, 6448 (1991).
[14] P. Kolodner, Phys. Rev. A **44**, 6466 (1991).
[15] B. L. Winkler and P. Kolodner, J. Fluid Mech. **240**, 31 (1992).
[16] M. Dubois, R. DaSilva, F. Daviaud, P. Bergé, and A. Petrov, EPL **8**, 135 (1989).
[17] F. Daviaud, P. Bergé, and M. Dubois, EPL **9**, 441 (1989).
[18] M. Dubois, P. Bergé, and A. Petrov, *The Geometry of Nonequilibrium*, NATO ASI Series, edited by P. Coullet and P. Huerre (Plenum, New York, 1990), Vol. 237, p. 227.
[19] J. Hegseth, J. M. Vince, M. Dubois, and P. Bergé, EPL **17**, 413 (1992).
[20] F. S. Merkt, R. D. Deegan, D. I. Goldman, E. C. Rericha, and H. L. Swinney, Phys. Rev. Lett. **92**, 184501 (2004).
[21] H. H. Rotermund, S. Jakubith, A. von Oertzen, and G. Ertl, Phys. Rev. Lett. **66**, 3083 (1991).
[22] K. J. Lee, W. D. McCormick, Q. Ouyang, and H. L. Swinney, Nature (London) **369**, 215 (1994).
[23] V. B. Taranenko, K. Staliunas, and C. O. Weiss, Phys. Rev. A **56**, 1582 (1997).
[24] H. R. Brand, P. S. Lomdahl, and A. C. Newell, Phys. Lett. A **118**, 67 (1986); Physica D **23**, 345 (1986).
[25] N. Akhmediev Ed, *Dissipative Solitons* (Springer, New York, 2008).
[26] N. Akhmediev, J. M. Soto-Crespo, and G. Town, Phys. Rev. E **63**, 056602 (2001).
[27] R. J. Deissler and H. R. Brand, Phys. Lett. A **146**, 252 (1990).
[28] S. Fauve and O. Thual, Phys. Rev. Lett. **64**, 282 (1990).
[29] W. van Saarloos and P. C. Hohenberg, Phys. Rev. Lett. **64**, 749 (1990).
[30] V. Hakim and Y. Pomeau, Eur. J. Mech. B/Fluids **10**, 137 (1991).
[31] B. A. Malomed and A. A. Nepomnyashchy, Phys. Rev. A **42**, 6009 (1990).
[32] R. J. Deissler and H. R. Brand, Phys. Rev. A **44**, R3411 (1991).
[33] R. J. Deissler and H. R. Brand, Phys. Rev. Lett. **72**, 478 (1994).
[34] P. Marcq, H. Chaté, and R. Conte, Physica D **73**, 305 (1994).
[35] V. V. Afanasjev, N. N. Akhmediev, and J. M. Soto-Crespo, Phys. Rev. E **53**, 1931 (1996).
[36] R. J. Deissler and H. R. Brand, Phys. Rev. Lett. **81**, 3856 (1998).
[37] O. Descalzi, M. Argentina, and E. Tirapegui, Int. J. Bifurcation Chaos Appl. Sci. Eng. **12**, 2459 (2002); Phys. Rev. E **67**, 015601(R) (2003).
[38] O. Descalzi, Physica A **327**, 23 (2003).
[39] O. Descalzi and E. Tirapegui, Physica A **342**, 9 (2004).
[40] J. M. Soto-Crespo, M. Grapinet, Ph. Grelu, and N. Akhmediev,

Phys. Rev. E **70**, 066612 (2004).
[41] O. Descalzi and H. R. Brand, Phys. Rev. E **72**, 055202(R) (2005).
[42] O. Descalzi, J. Cisternas, and H. R. Brand, Phys. Rev. E **74**, 065201(R) (2006).
[43] O. Descalzi, H. R. Brand, and J. Cisternas, Physica A **371**, 41 (2006).
[44] H. R. Brand, O. Descalzi, and J. Cisternas, AIP Conf. Proc. **913**, 133 (2007).
[45] O. Descalzi, J. Cisternas, P. Gutiérrez, and H. R. Brand, Eur. Phys. J. Spec. Top. **146**, 63 (2007).
[46] O. Descalzi, J. Cisternas, D. Escaff, and H. R. Brand, Phys. Rev. Lett. **102**, 188302 (2009).
[47] P. Gutiérrez, D. Escaff, S. Pérez-Oyarzún, and O. Descalzi, Phys. Rev. E **80**, 037202 (2009).
[48] H. Sakaguchi, Prog. Theor. Phys. **86**, 7 (1991).
[49] H. Sakaguchi, Prog. Theor. Phys. **89**, 1123 (1993).
[50] O. Descalzi, P. Gutiérrez, and E. Tirapegui, Int. J. Mod. Phys. C **16**, 1909 (2005).
[51] O. Descalzi and H. R. Brand, Prog. Theor. Phys. **119**, 725 (2008).
[52] O. Descalzi and H. R. Brand, Phys. Rev. E **81**, 026210 (2010).
[53] J. M. Soto-Crespo, N. Akhmediev, and A. Ankiewicz, Phys. Rev. Lett. **85**, 2937 (2000).
[54] S. T. Cundiff, J. M. Soto-Crespo, and N. Akhmediev, Phys. Rev. Lett. **88**, 073903 (2002).
[55] N. Akhmediev and J. M. Soto-Crespo, Phys. Lett. A **317**, 287 (2003).
[56] N. Akhmediev and J. M. Soto-Crespo, Phys. Rev. E **70**, 036613 (2004).
[57] O. Descalzi, Phys. Rev. E **72**, 046210 (2005).
[58] O. Descalzi, S. Martinez, and E. Tirapegui, Chaos, Solitons Fractals **12**, 2619 (2001).
[59] Y. Hayase, O. Descalzi, and H. R. Brand, Phys. Rev. E **69**, 065201(R) (2004).
[60] O. Descalzi, Y. Hayase, and H. R. Brand, Int. J. Bifurcation Chaos Appl. Sci. Eng. **14**, 4097 (2004).
[61] O. Descalzi, Y. Hayase, and H. R. Brand, Phys. Rev. E **69**, 026121 (2004).
[62] Y. Hayase, O. Descalzi, and H. R. Brand, Physica A **356**, 19 (2005).